Journal of Interfaces, Thin films, and Low dimensional systems 8 (1) Summer and Autumn (2024) 789-801

The effect of the geometrical parameters and composing materials type on the bandgap width of two-dimensional phononic crystals

Scientific research paper

Parisa Mahmoudi[1], *Mehdi Solaimani*[2*]

[1]*Department of Electrical and Computer Engineering, Qom University of Technology, Qom, Iran*

[2]*Department of Physics, Qom University of Technology, Qom, Iran*

ARTICLE INFO

Article history:
Received 10 August 2024
Revised 14 November 2024
Accepted 18 November 2024
Available online 18 December 2024

Keywords
Phononic crystal
Bandgap
Lattice constant

ABSTRACT

In this article, the bandgap of the two-dimensional phononic crystal with some holes in a square plane was studied using the finite element method by the Comsol software. The holes are made of both solids and liquids simultaneously in our phononic crystals that are less studied so far. We examined the fixed lattice constant while the cavity radius changes and vice versa. We found larger bandgap widths when the cavity was made of nickel metal while the surrounding media is water. We observed that the system with higher sound speed possesses a more significant band gap. At higher temperatures, we will have a higher sound speed, and thus, a higher bandgap width. We have a smaller bandgap when the holes are covered by metal. The main aim of the manuscript was to find an optimum structure that has a phononic crystal with largest passible phononic band gap for filtering property applications. In this way, we have considered the effect of different parameters such as lattice constant, composing materials, phononic crystal geometry, and temperature on the phononic bandgap width.

1 Introduction

In the last decade, studying the phononic crystals has grown exponentially [1-2]. For an excellent review one may see [43]. These; structures are periodic composite materials similar to elastic and acoustic photonic crystals [3-4]. This growing interest is driven not only by potential applications such as novel acoustic devices, but also by the rich physics governing the propagation of elastic and acoustic waves in the periodic media [5-7]. In; addition, ultrasonic and acoustic techniques, along with powerful theoretical approaches, can provide unique advantages for the direct investigation of wave phenomena in these systems. So; far, most of the studies have focused on the existence of phononic bandgaps, which occur due to the Bragg scattering when the wavelength is comparable to the lattice constants. This, also leads to creation of the frequency bands at which wave propagation is prohibited [1, 5, 8-9]. In Refs. [35,36], the theoretical and experimental studies on the use of phonon crystal plates are considered. In the band structure of one and two-dimensional crystal phonon structures, the band gap is sensitive to the thickness between the plane and the lattice constant [37]. Recently; phononic crystals have entered the world of micro-electromechanical systems (MEMS) thanks to their ability to manipulate the propagation of elastic waves [38] .The phononic crystal has attracted much attention because the size of the phononic crystal is larger than the photonic crystal due to the relation

*Corresponding author.
Email address: Solaimani.mehdi@gmail.com
DOI: 10.22051/jitl.2024.47976.1111

between the wavelength of sound and light [39]. The Phononic crystals provide unique band structures for propagating sound waves [40].

The acoustic crystals are used in elastic waveguide transducers to control their beam patterns [41]. The Phononic crystals are sound metamaterials that are designed to manipulate sound when its wavelength is in the order of the constant magnitude of the crystal lattice [42]. The dispersion properties of acoustic crystals can be used to manipulate the acoustic impedance of a material and to engineer the delay frequency response of time domain signal processing circuits. [30].

Understanding how sizeable full band gaps can be achieved in physically realizable materials and describing the wave propagation mechanism at gap frequencies have significantly progressed [9]. However, relatively little attention has been paid to investigating how periodicity affects wave propagation over a wide range of frequencies outside the band gaps. At; low frequencies, a continuous approximation can accurately predict the motion velocities. In this frequency range, the low-frequency phonons properties in common atomic crystals have been systematically studied [10]. Recently; low-frequency two-dimensional acoustic crystal devices have been developed for airborne sound [6] and analyzed theoretically [11].

The first complete phononic band was demonstrated in [12-13]. Since then, much progress has been made in the theoretical analysis and representation of acoustic crystals [14-15] and acoustic crystal-based devices such as waveguides; [16-18], filters [19-20], and acoustic resonance [21]. Until recently, the physical realization of acoustic crystals are largely limited to the manual assembly of balls or rods in water, epoxy, or air. [22-23]. In 2005, Liu et al. investigated the frequency band structure in a two-dimensional phononic crystal consisting of a six-species (hexagonal) lattice including steel cylinders in an aired substrate [24]. In 2006, Eswar et al. showed the inversion of the ferroelectric domain on z-cut LiNbO using electron beam irradiation. They obtained the inversion of the domains by obtaining the thickness of the two-dimensional blue phonon holes in the +z and -z direction, and the presence of the acoustic band gap in about 200 MHz [25].

In 2008, Xiao Zhu and Chuanzeng Zhang, using the wave equation, proved that the material parameters directly determine the acoustic band gaps. They used the plane wave expansion method to calculate the band gaps. Their results show that the maximum band gap is related to the mass density ratio [26]. In 2009, Profanser et al. experimentally and numerically investigated the interaction between ultra-high frequency sound waves with periodic microstructures composed of copper lines embedded in silicon oxide and two-dimensional acoustic crystals consisting of air-filled holes. Experimental results obtained with ultrashort pulsed optical excitation and interferometric detection are compared with time-domain finite-element simulations. A good agreement between the simulation and the experiment was obtained. [27] In 2010, Mohammadi et al. stated that the phononic crystals with periodic changes in their elastic properties, if properly designed, can exhibit a frequency range in which the propagation of elastic waves is wholly prohibited. In this frequency range, the elastic energy of the crystal phonon structure can be limited and manipulated [28]. In; 2011, Zhao et al. used lattice configurations to create different band gap effects and calculated the phononic crystal band structures of square lattice and honeycomb steel rods in water by the wave plane expansion method [29].

Kim and Rakich (2013) studied the scattering properties of phononic crystals formed from thin suspended aluminum nitride plates that could be used to manipulate the acoustic impedance of a material and engineer the delay-frequency response of the time-domain signal processing circuits [30].

Ya et al. (2015) used phononic crystals to trap acoustic energy and reduce the anchor loss of AT- cut quartz resonators. The resonant response of an AT-cut quartz resonator without an acoustic crystal was first calculated. A square-lattice phononic crystal plate, made of an AT-cut quartz plate with air holes, was analyzed and designed to have a complete bandgap covering the resonant frequency of the quartz resonator. Finally, the mode shape and impedance of the quartz resonator with three rows of phononic crystals were calculated to evaluate the isolation performance of the acoustic crystals [31]. In 2017, Deng and Jing investigated a flowless quasi-spin- based acoustic topological insulator. Region folding, a strategy originating from photonic crystals, is used to form double Dirac cones in phononic crystals. The symmetry of the phononic crystal lattice is broken by adjusting the size of the center "atom" of the unit cell to open a

negligible topological gap. The one-way propagation of strong sound is shown numerically. This provides a flexible approach for realizing the topological acoustic insulators that are promising for applications such as noise control and waveguide design [32]. In 2018, Sediqi and Joshua presented an aluminum nitrate-on-silicon waveguide; with a wide acoustic bandgap phononic crystal which increases the quality factor by four times [33]. In 2019, Bao et al. investigated the conventional approaches to phononic crystals. They presented new structures using a reflection strategy based on integrated phononic crystal, which reduced the anchor loss and improved the quality factor. These structures suit for up to frequency of 10 MHz MEMS resonators [34].

In the current work, the band structure of the two-dimensional phononic crystal of circular holes inside the square plane has been investigated for different materials of solids and liquids. The aim is to find a larger bandgap width for each material.

2 Solution method

In the powerful Comsol multiphysics software, we used the acoustic module. The aim was to obtain the band structure for the desired geometry with different materials. The cavity is made of magnesium, nickel, and aluminum with the speeds of sound 5770, 3000 and 6410 while the temperature was 293.15 Kelvin. Water is considered at different conditions with the speed of sound 1500.99 and temperature 308.15, the speed of sound 1522.26 and the temperature 313.15, the speed of sound of 1534.69 and the temperature of 318.15. The sound speed of 1563.40, and temperature of 298.15 for hexane; and the speed of sound of 1089.85 and the temperature of 298.15 for heptane are used. We did not include other parameters in the software.

First, we consider infinite arrays of holes in a square plane containing solid and liquid materials (the holes are once made of liquids and once made of solids). Their band structure is calculated using the finite element method, which is developed in the framework of Comsol software. Calculations are done using the finite element method. The basis of work in this method is to simplify the equations to ordinary differential equations, which are solved by numerical methods such as Euler schema. In the calculations using the Comsol software, in the finite element framework in the first Brillouin zone, eigenfrequencies are obtained using the acoustic module. By choosing the sound speed related to the material inside the cavity, making periodic squares containing the cavities and choosing the appropriate mesh size, the band structures are calculated.

A; phononic crystal in a 2D square array of the unit cell is used as the basis for the calculations.

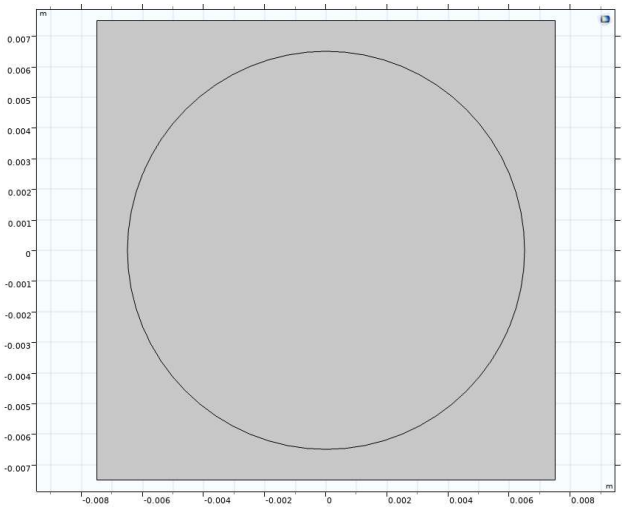

Figure 1. Phonon crystal unit cell.

According to the Floquet-Bloch theorem, the pressure distribution relationship p for the nodes located on the boundary of the unit cell can be expressed as

$$\rho(\vec{x} + \overrightarrow{a_1} + \overrightarrow{a_2}) = \rho(x)\exp\left[i\left(k_x a_1 + k_y a_2\right)\right]$$

where the position of the x vector in the unit cell $\vec{k} = \left(k_x . k_y\right)$ is the Bloch wave vector.

First, we apply Neumann boundary conditions. This is required on boundaries where the pressure p is controlled by a periodic boundary condition. A phase relation is then used at the unit boundary to define the boundary conditions between adjacent units. This phase relationship is related to the wave number of the incident wave in the periodic structure. The regular boundary conditions shorten the 2D simulation plane in the x and y directions by reducing the system to a unit cell. An ideal crystal is infinitely periodic, so the regular boundary condition ensures that the finite simulation space of a finite crystal is

infinite in the x direction and pattern. Pressure components at all edges of the computational domain are transferred to opposite edges of the field by periodic boundary conditions.

In the first case, we used the nickel metal inside the hole and the water around the hole. Then, we increased the lattice constant from 13 mm to 24 mm and calculated the width of the bandgap. The results are shown in Fig. 2. When the hole radius is fixed at 6.5 mm, as the phononic crystal lattice constant increases, for the case that the hole is made of nickel metal while surrounded by water, the gap size is smaller. Then by filling the cavity with the solids such as silica, the width of the bandgap becomes greater. We note that the sound speed is also higher in silica. Thus, it has a direct relationship with the bandgap width.

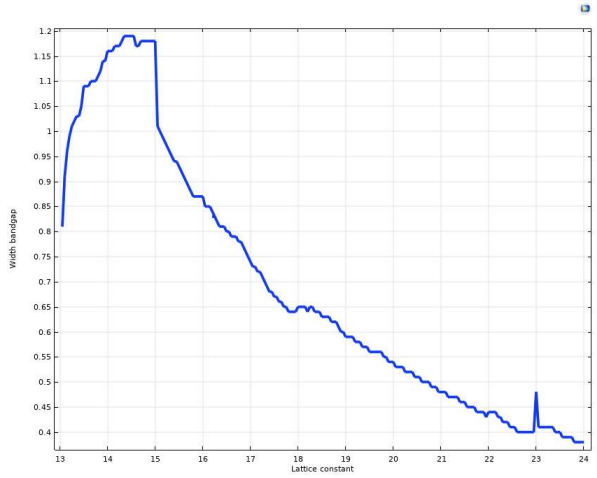

Figure 2. Bandgap width of phononic crystal as a function of the lattice constant from 13 to 24 mm. Inside; the cavity is made of nickel metal that surrounded by water with a cavity radius of 6.5 mm.

The sound pressure when the lattice constant increases are illustrated in Fig. 3. The radius of the cavity is 6.5 mm, and the hole is made of nickel metal which is surrounded by water. Figure 3c is related to the grid constant of 15 mm. This could be due to the numerical uncertainty that is unavoidable.

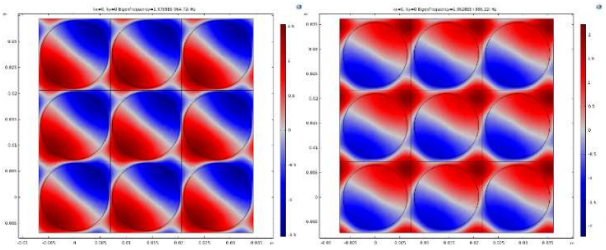

(a) (b)

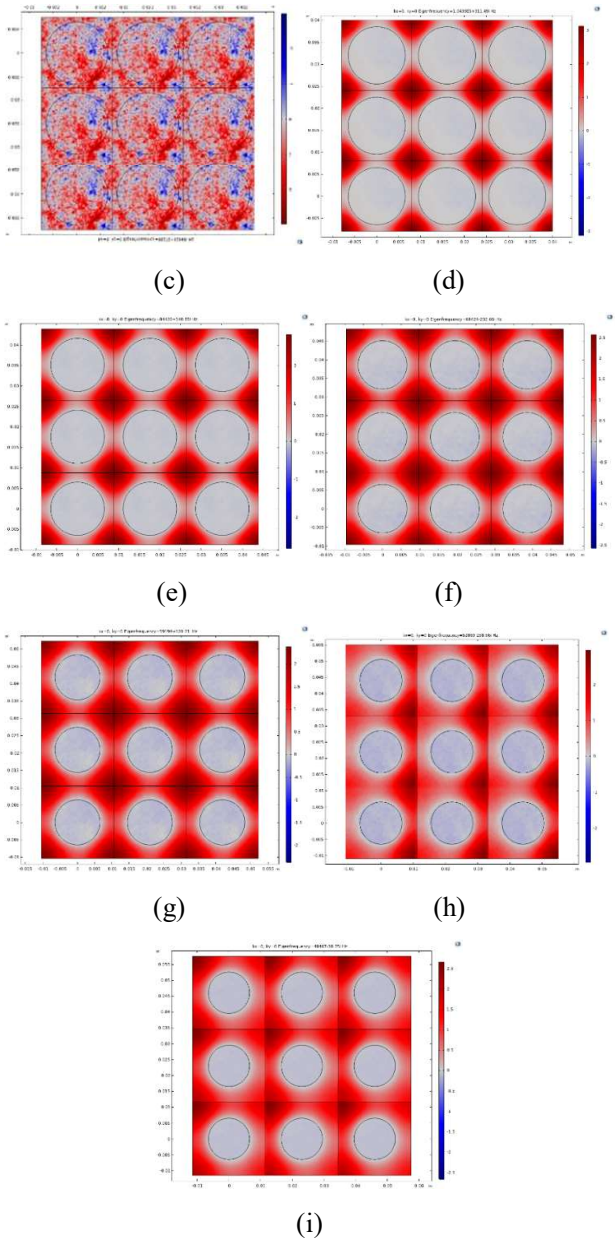

(c) (d)

(e) (f)

(g) (h)

(i)

Figure 3. (a): The sound pressure when the cavity is made of nickel metal and surrounded by water with a cavity radius of 6.5 mm and the lattice constant of 13.70 mm. Panels (b) to (i) are the same as the panel (a) but for lattice constants 14.45, 15.00, 16.00, 17.55, 19.30, 20.90, 22.00, and 23.00 mm, respectively.

The frequency range is 100 to 300 kHz. The maximum gap width occurs for a lattice constant of 15 mm. Then, we filled the holes with some liquids at room temperature while the circumference was made from nickel metal with a diameter of 6.5 mm. According to Fig. 4, the bandgap width is proportional to the sound speed. The higher the sound speed, the greater the gap width. The sound speeds are arranged as $C_{Hexane} < C_{Heptane} < C_{H2o}$. According to Fig. 4, the gap width is higher when we use water [36].

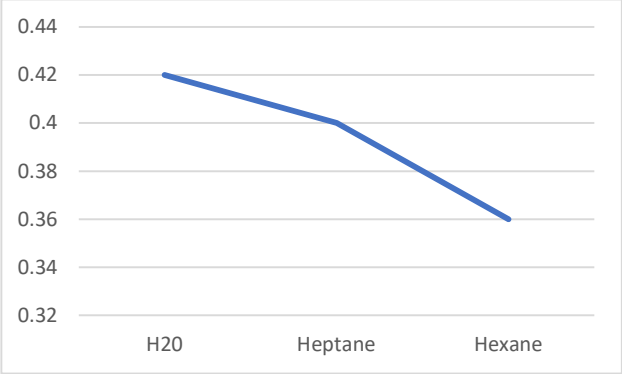

Figure 4. The bandgap width when filling the cavity with some liquids. The holes are immersed in the nickel metal matrix. The cavity radius is 6.5 mm, and the lattice constant is 15 mm.

The sound pressure when the cavity liquid changes while the holes are immersed in nickel metal is shown in Fig. 5.

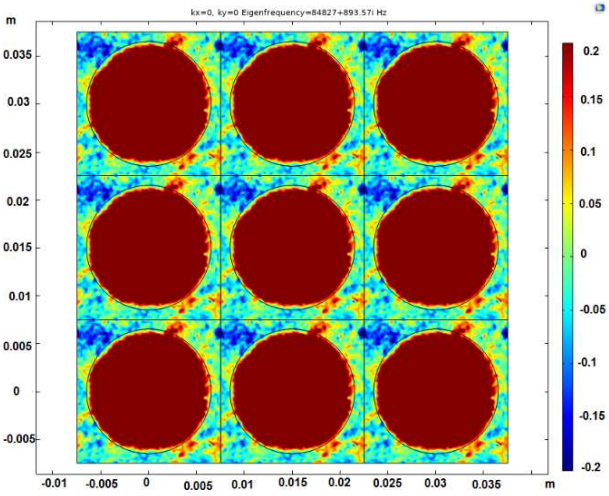

(a)

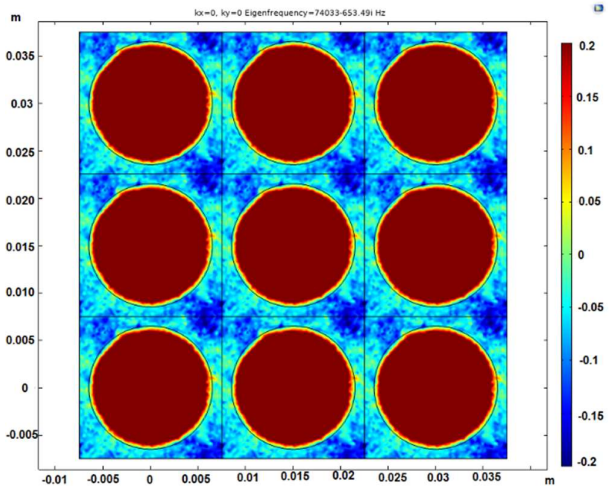

(b)

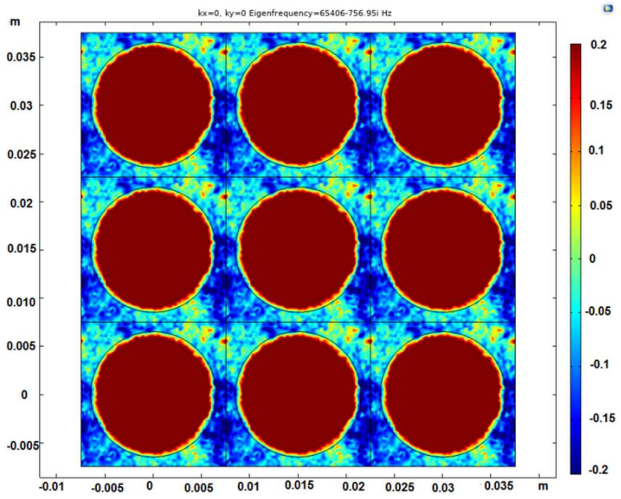

(c)

Figure 5. (a): The sound pressure inside the cavity is filled with water while around the holes is made of nickel metal. The cavity radius is 6.5 mm and the lattice constant is 15 mm. In panels (b) and (c), the holes are filled with heptane and hexane, respectively.

The frequency range is from 10 kHz to 20 kHz. From the sound pressure contour plots, we see that, when the cavity is made of water, more sound is propagated throughout the structure in the mentioned frequency ranges. Then we filled the holes with some solids at room temperature. The circumference is made of nickel metal. The hole radius is 6.5 mm. Figure 6 shows the bandgap width for the mentioned solids. The; maximum bandgap width is also due to the silica [37].

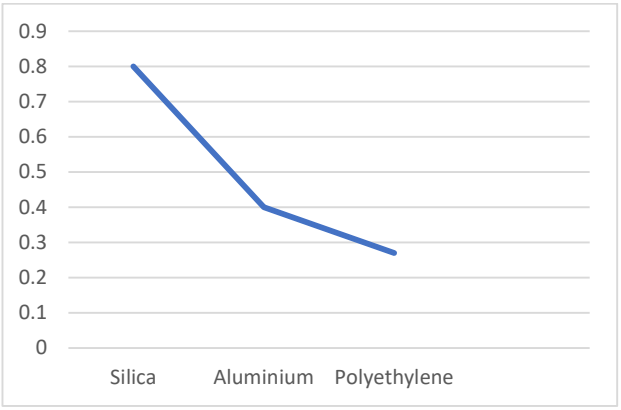

Figure 6. The bandgap width when the hole is made of some solids. The circumference is made of nickel metal, and the hole's radius is 6.5 mm. The lattice constant is 15 mm.

The sound pressure for some solids in the cavity while the surrounding matrix is the nickel metal is presented in Fig. 7.

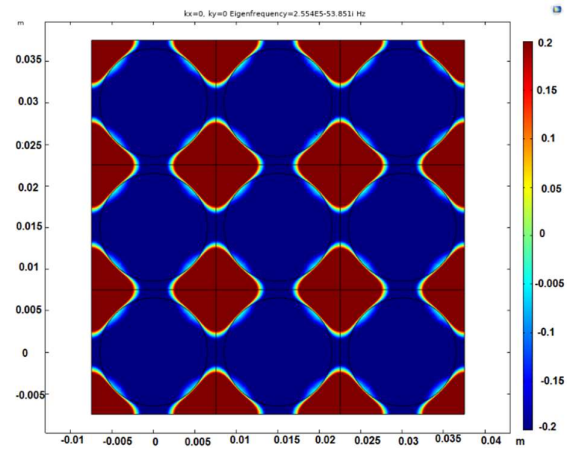

(a)

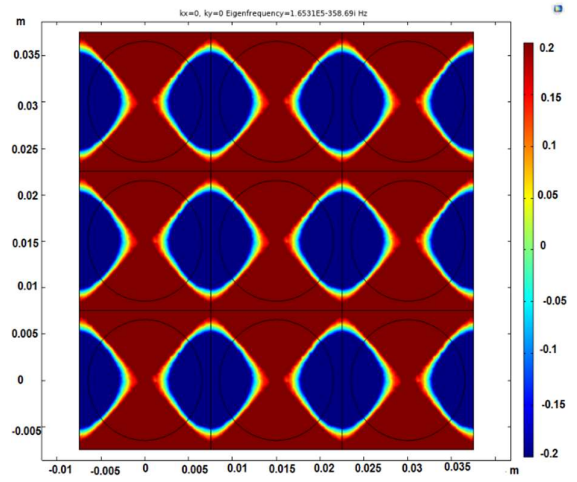

(b)

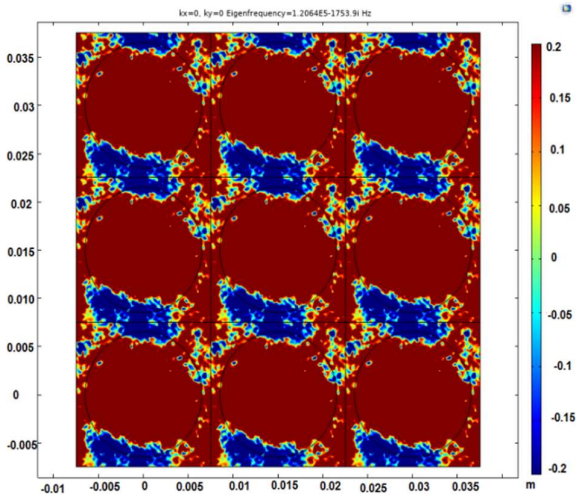

(c)

Figure 7. (a): The sound pressure when the cavity is made of silica with surrounding nickel metal. The; hole's radius is 6.5 mm, and the lattice constant is 15 mm. Panels (b) and (c) are the same as panel (a), but the cavity is made of aluminum and polyethylene, respectively.

When the hole is made of water, and the holes are surrounded by nickel metal, the bandgap width as a function of the radius of the hole is shown in Fig. 8. Different temperatures are compared here. There is no gap at the lower radii. As the temperature increases, the transverse sound speed in water also increases, and we have a larger bandgap.

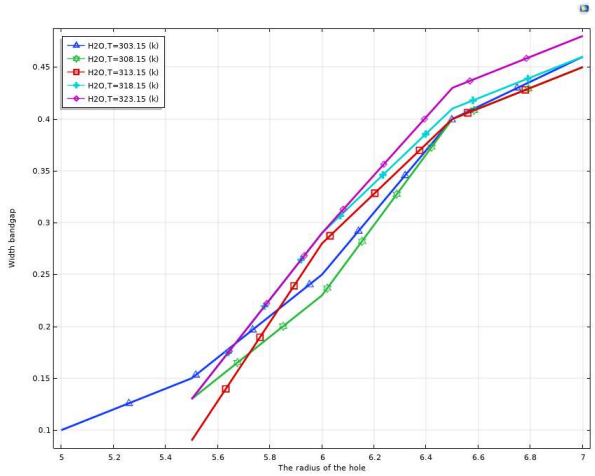

Figure 8. The bandgap width as a function of the cavity radius for different temperatures when the cavity is filled with water, and surrounded by nickel metal.

nickel metal.

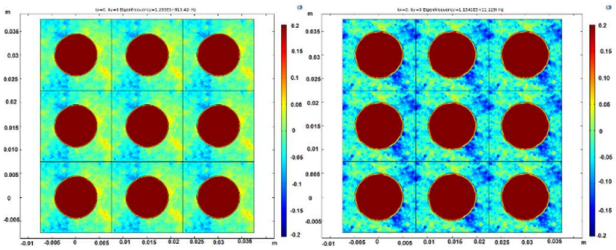

(a) (b)

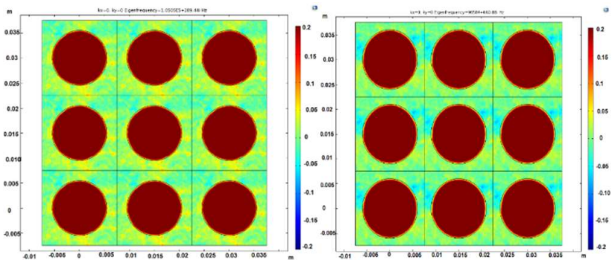

(c) (d)

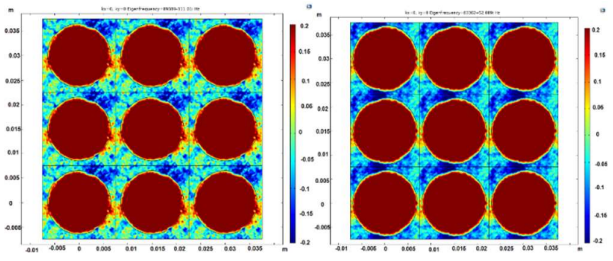

(e) (f)

Figure 9. (a): The sound pressure when the cavity is filled with water and the surrounding media is made of nickel metal while the radius is 4.5 mm and the temperature is 303.15 K. Panels (b) to (f) are the same as panel (a) but for hole radiuses 5, 5.5, 6, 6.5, and 7 mm, respectively.

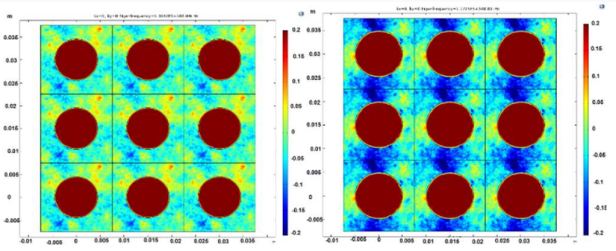

(g) (h)

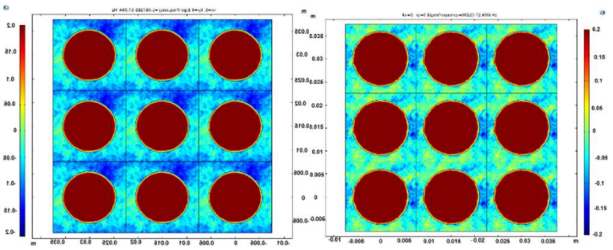

(i) (j)

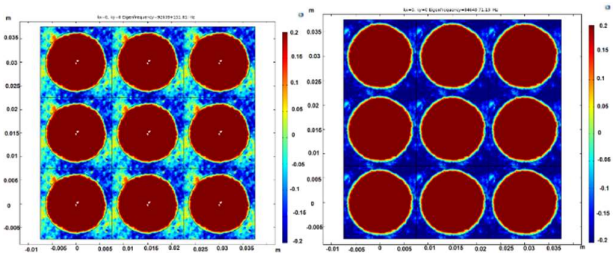

(k) (z)

Figure 10. (g): The sound pressure when the cavity is made of water with surrounding nickel metal. The hole radius is 4.5 mm, and the temperature is 308.15 K. Panel (h) is the same as panel (g), but the radius of the hole is 5, 5.5, 6, 6.5, and 7 mm, respectively.

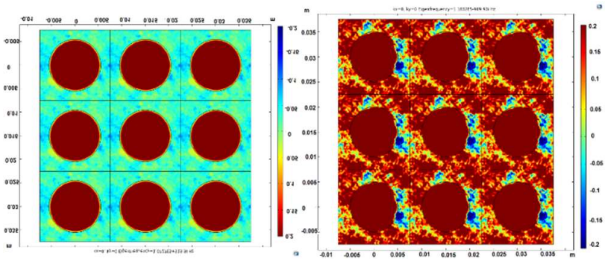

(a1) (b1)

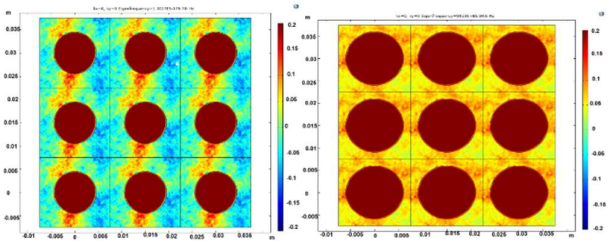

(c1) (d1)

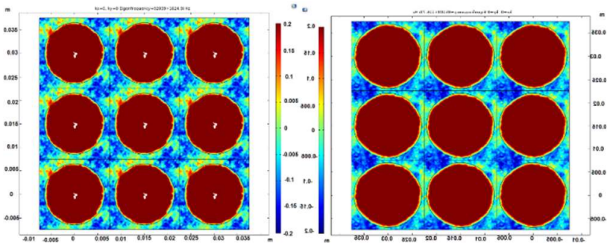

(e1) (f1)

Figure 11. (a1): The sound pressure when the cavity is made of water with surrounding nickel metal. The hole radius is 4.5 mm, and the temperature is 313.15 K. Panel (b1) are the same as panel (f1) but the radius of the hole is 5, 5.5, 6, 6.5, and 7 mm, respectively.

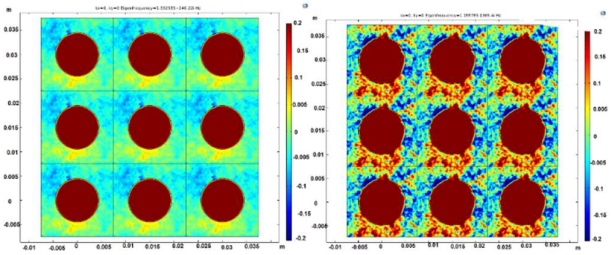

(a2) (b2)

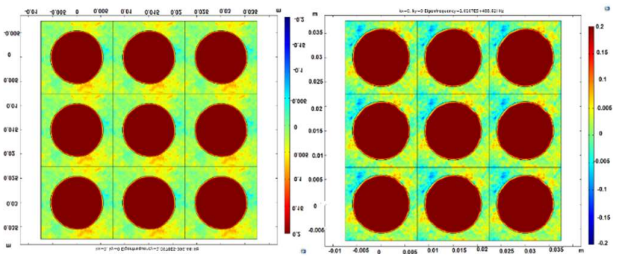

(c2) (d2)

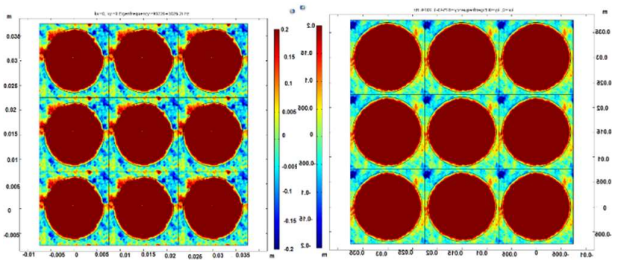

(e2) (f2)

Figure 12. (a2): The sound pressure when the cavity is made of water with surrounding nickel metal while the hole radius is 4.5 mm and the temperature is 318.15 K. Panels (b2) is the same as panel; (f2), but for the radius of the hole 5, 5.5, 6, 6.5, and 7 mm, respectively.

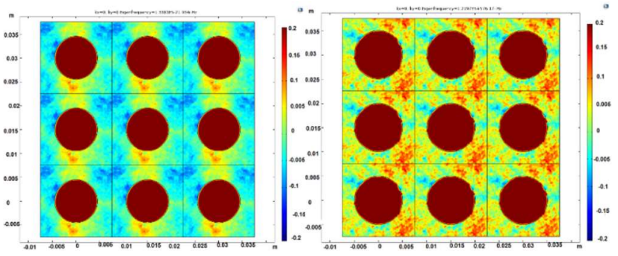

(a3) (b3)

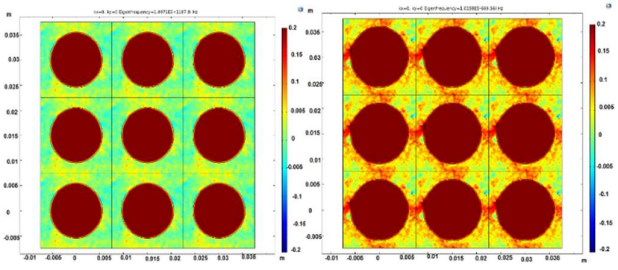

(c3) (d3)

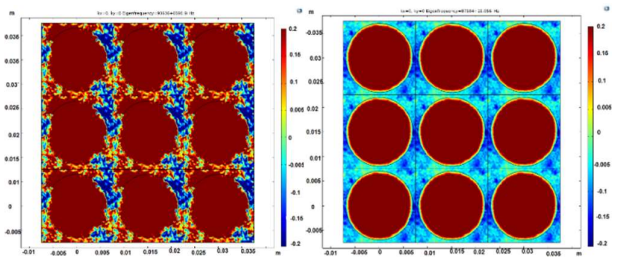

(e3) (f3)

Figure 13. (a3): The sound pressure when the cavity is made of water with surrounding nickel metal while the hole radius is 4.5 mm and the temperature is 323.15 K. Panels (b3) are the same as panel; (f3) but the radius of the hole 5, 5.5, 6, 6.5, and 7 mm, respectively.

According to the sound pressure contour plots for water at different temperatures, when the radius of the hole increases, it is evident that at the temperature of 323.15 K, the sound propagation depends on the hole radius. At higher radii, more sound is trapped inside the structure, and the gap width is more considerable.

The gap width when the hole radius increases for different materials and the lattice constant of 15 mm is shown if Fig. 14. According to this figure, when the hole is made of the nickel metal that is surrounded by water, for a larger hole radius, an array of holes in the lattice constant of 15 mm are closer to each other.

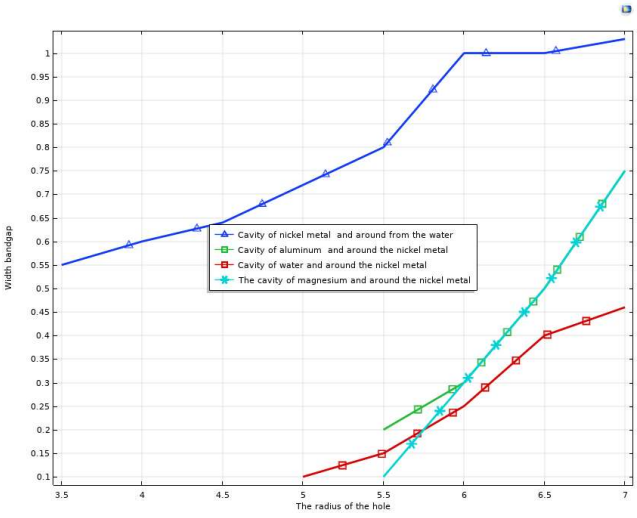

Figure 14. The bandgap width as a function of the hole radius when the cavity is made of nickel metal that is surrounded by the water, the cavity is made of aluminum metal that is surrounded by nickel metal, the hole is made of the water that is surrounded by nickel metal, and the hole is made of the magnesium that is surrounded by the nickel metal.

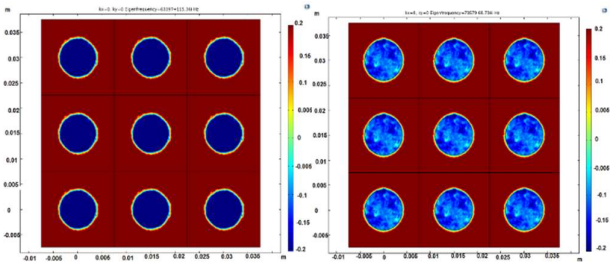

(a) (b)

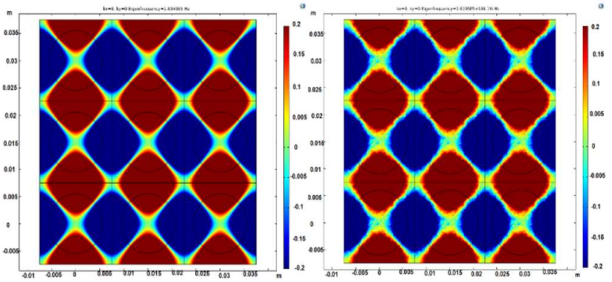

(i) (j)

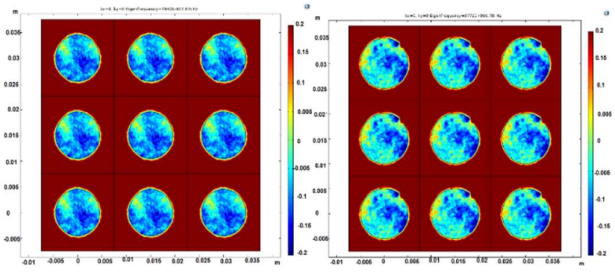

(c) (d)

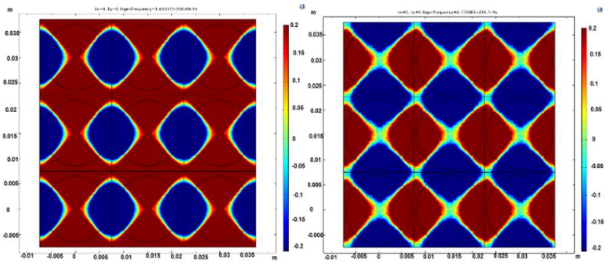

(k) (l)

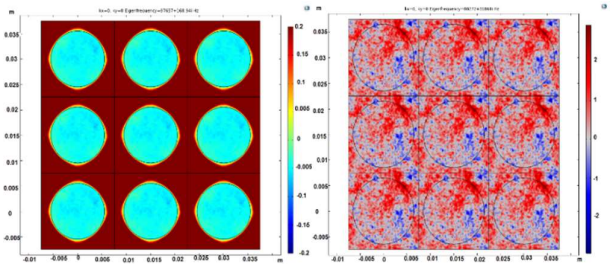

(e) (f)

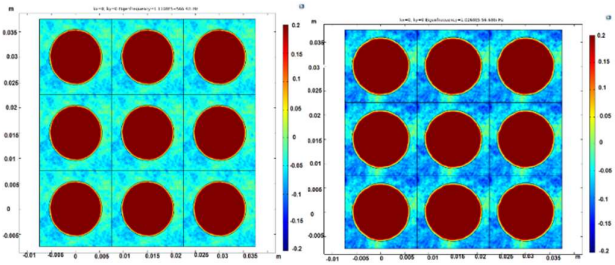

(m) (n)

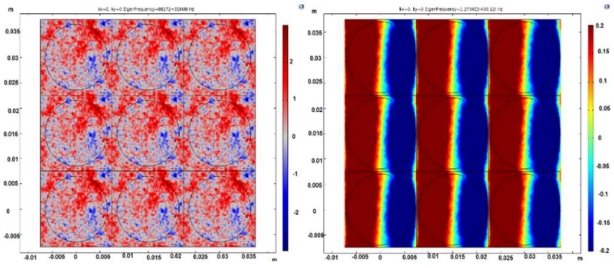

(g) (h)

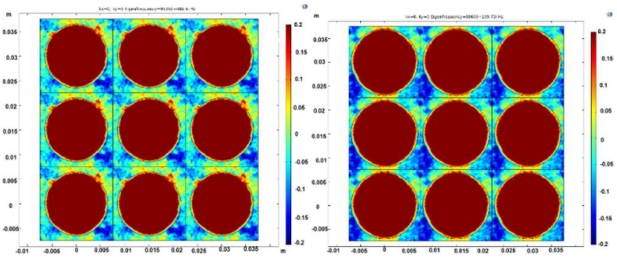

(o) (p)

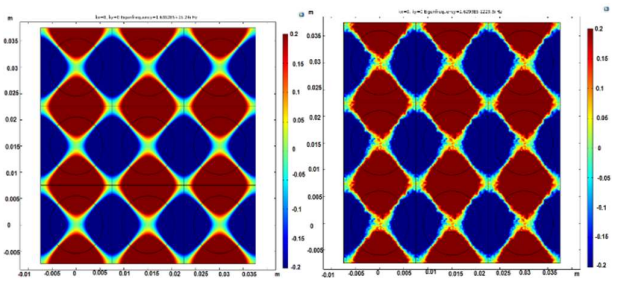

(p) (q)

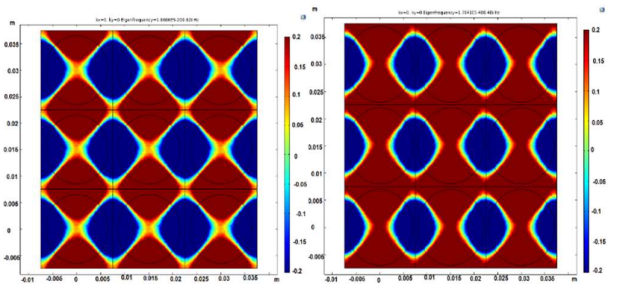

(r) (s)

Figure 15. (a): The sound pressure when the cavity is made of nickel metal that is surrounded by the water with a cavity radius of 3.5 mm and a lattice constant of 15 mm. Panels (b) to (h) are the same as panel (a) but for the hole's radiuses 4, 4.5, 5, .55, 6, 6.5, and 7 mm, respectively. (i): The acoustic pressure when the cavity is made of aluminum metal surrounded by the nickel metal with a cavity radius of 5.5 mm and a lattice constant of 15 mm. Panel (j) to (l) are the same as panel (i), but for the hole's radiuses 6, 6.5, and 7 mm, respectively. (m): the sound pressure when the cavity is made of the water that is surrounded by the nickel metal with a cavity radius of 5.5 mm and a lattice constant of 15 mm. Panel (n) to (p) are the same as the panel; (m) but for the hole's radiuses 6, 6.5, and 7 mm, respectively. (q): the acoustic pressure when the cavity is made of magnesium that is surrounded by nickel metal with a cavity radius of 5.5 mm and a lattice constant of 15 mm. Panel (r) to (t) are the same as panel (q), but for the hole's radiuses 6, 6.5, and 7 mm, respectively.

For more illustration purposes, the band structures of systems with different lattice constants are shown in Fig. 16.

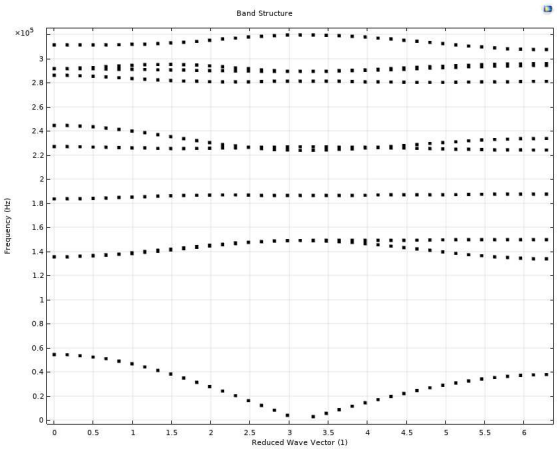

(a)=13mm

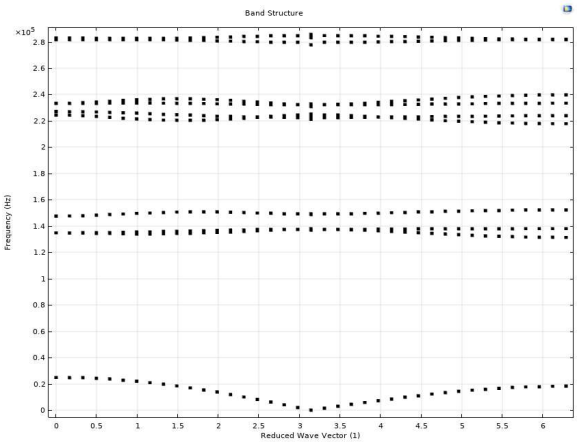

(b)=14mm

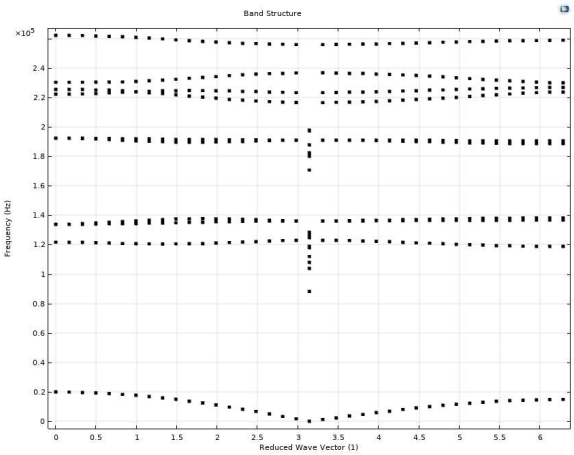

(c)=15mm

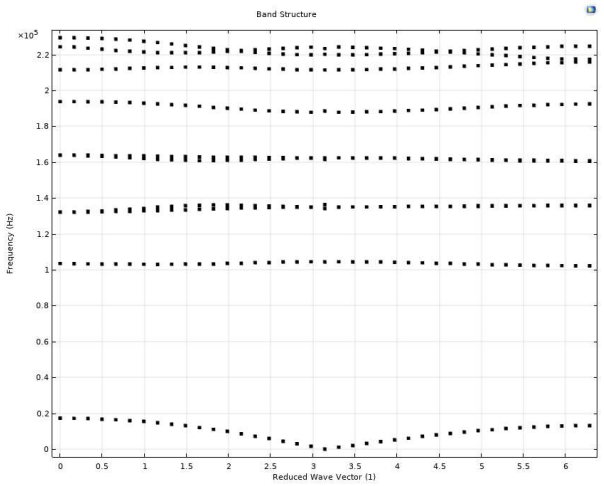

(d)=16mm

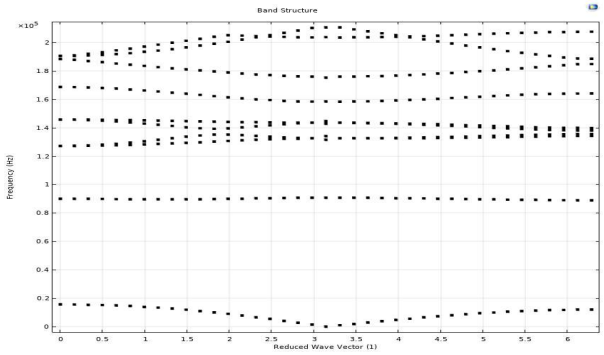

(e)=17mm

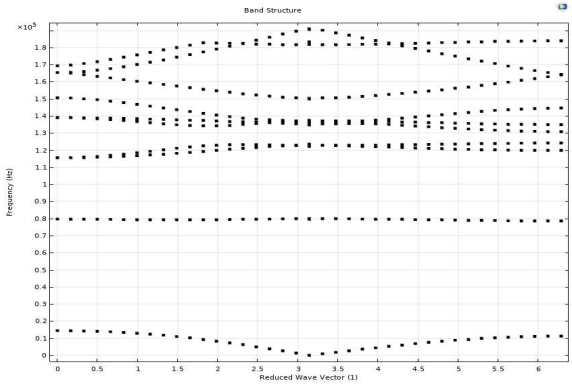

(f)=18mm

Figure 16. Band structures of systems with different lattice constants.

3 Discussion and conclusions

The phononic crystal with lattice constants in the range of 14-15 mm has maximum bandgap width when the cavity is made of nickel metal and is surrounded by water. We filled the holes with different solids and liquids. We observed that the system with higher sound speed possesses a more significant band gap. Then we examined the cavity of water at different temperatures. At higher temperatures, we will have a higher sound speed, and thus, a higher bandgap width. When the lattice constant is 15 mm, and the cavity is made of nickel metal before surrounded by water, we have a larger bandgap. However, we have a smaller bandgap when the holes are covered by metal.

References

[1] M. M. Sigalas, "Defect states of acoustic waves in a two-dimensional lattice of solid cylinders." Journal of Applied Physics, **84** (1998) 3026.

[2] S. Yang, J. H. Page, Z. Liu, M. L. Cowan, C. T. Chan, P. Sheng "Focusing of sound in a 3D phononic crystal." Physical review letters, **93** (2004) 024301.

[3] E. Yablonovitch, "Inhibited spontaneous emission in solid-state physics and electronics." Physical review letters, **58** (1987) 2059.

[4] C. Luo, S. G. Johnson, J. D. Joannopoulos, and J. B. Pendry, "Subwavelength imaging in photonic crystals." Physical Review B, **68** (2003) 045115.

[5] J. O. Vasseur, P A Deymier, B. Chenni, B. Djafari-Rouhani, L. Dobrzynski, D. Prevost "Experimental and theoretical evidence for the existence of absolute acoustic band gaps in two-dimensional solid phononic crystals." Physical Review Letters, **86** (2001) 3012.

[6] F. Cervera, L. Sanchis, J. V. Sánchez-Pérez, R. Martinez-Sala, C. Rubio, F. Meseguer, C. López, D. Caballero, J. Sánchez-Dehesa "Refractive acoustic devices for airborne sound." physical review letters, **88** (2001) 023902.

[7] N. Garcia, M. Nieto-Vesperinas, E. V. Ponizovskaya, and M. Torres. "Theory for tailoring sonic devices: Diffraction dominates over- refraction." Physical Review E, **67** (2003) 046606.

[8] M. Torres, F. R. Montero de Espinosa, and J. L.

Aragon. "Ultrasonic wedges for elastic wave bending and splitting without requiring a full band gap." Physical Review Letters, **86** (2001) 4282.

[9] Y. Suxia, J. H. Page, Z. Liu, M. L. Cowan, C. T. Chan, and P. Sheng. "Focusing of sound in a 3D phononic crystal." Physical review letters, **93** (2004) 024301.

[10] Drumheller, S. Douglas Introduction to wave propagation in nonlinear fluids and solids. Cambridge; University Press, 1998.

[11] Gupta, C. Bikash, and Z. Ye "Theoretical analysis of the focusing of acoustic waves by two-dimensional sonic crystals." Physical Review E, **67** (2003) 03660.

[12] D. Espinosa, F.R. Montero, E. Jimenez, and M. Torres "Ultrasonic band gap in a periodic two-dimensional composite." Physical Review Letters, **80** (1998) 1208.

[13] W. M. Robertson, and J. F. Rudy "Measurement of acoustic stop bands in two-dimensional periodic scattering arrays." The Journal of the Acoustical Society of America **104** (1998) 694.

[14] M. Toyokatsu. "Sonic crystals and sonic waveguides." Measurement Science and Technology, **16** (2005) R47.

[15] Y. Suxia, J. H. Page, Z. Liu, M. L. Cowan, C. T. Chan, and P. Sheng. "Ultrasound tunneling through 3D phononic crystals." Physical review letters, **88** (2002) 104301.

[16] O. Jerome, A-C. Hladky-Hennion, B. Djafari-Rouhani, F. Duval, B. Dubus, Y. Pennec, and P. A. Deymier. "Waveguiding in two-dimensional piezoelectric phononic crystal plates." Journal of applied physics, **101** (2007) 114904.

[17] A. Khelif, A. Choujaa, S. Benchabane, B. Djafari-Rouhaniand, V. Laude, "Guiding and bending of acoustic waves in highly confined phononic crystal waveguides;" Applied physics letters, **84** (2004) 4400.

[18] M. Torres, F. R. Montero de Espinosa, and J. L. Aragon. "Ultrasonic wedges for elastic wave bending and splitting without requiring a full band gap." Physical Review Letters, **86** (2001) 4282.

[19] A. Khelif, A. Choujaa, B. Djafari-Rouhani, M. Wilm, S. Ballandras, and V. Laude " Trapping and guiding of acoustic waves by defect modes in a full-band-gap ultrasonic crystal" Physical Review B, **68** (2003) 214301.

[20] F. Van Der Biest, A. Sukhovich, A. Tourin, J. H. Page, B. A.Van Tiggelen, Z. Liu, and M. Fink, "Resonant tunneling of acoustic waves through a double barrier consisting of two phononic crystals." Europhysics Letters, **71** (2005) 63.

[21] S. Jinjie, S. Chin, S. Lin, and T. Jun Huang; "Wide-band acoustic collimating by phononic crystal composites." Applied Physics Letters, **92** (2008) 111901.

[22] J. O. Vasseur, P. A. Deymier, B. Chenni, B. Djafari-Rouhani, L. Dobrzynski, and D. Prevost, "Experimental and theoretical evidence for the existence of absolute acoustic band gaps in two-dimensional solid phononic crystals." Physical Review Letters, **86** (2001) 3012.

[23] F. L. Hsiao, A. Khelif, H. Moubchir, A. Choujaa, C. C. Chen, and V. Laude, "Complete band gaps and deaf bands of triangular and honeycomb water-steel phononic crystals." Journal of applied physics, **101** (2007) 044903.

[24] P. A. Deymier, B. Merheb, J. O. Vasseur, A. Sukhovichand, J. H. Page, "Focusing of acoustic waves by flat lenses made from negatively refracting two-dimensional phononic crystals." Revista mexicana de física, **54** (2008) 74.

[25] M. B. Assouar, B. Vincent, H. Moubchir, O. Elmazria, A. Khelif, and V. Laude, "Domains Inversion in LiNbO3 Using Electron Beam Irradiation for Phononic Crystals." 15th IEEE international symposium on the applications of ferroelectrics. IEEE, 2006.

[26] Z. Xiao-Zhou, Y. S. Wang, and C. Zhang; "Essential role of material parameters on the band gaps of phononic crystals." IEEE; Ultrasonics Symposium. IEEE, 2008

[27] I. A. Veres, D. M. Profunser, O. B. Wright, O. Matsuda, and U. Lang, "Real-time simulations and experiments on ultrahigh frequency surface waves in micro-structured phononic crystals." IEEE International Ultrasonics Symposium. IEEE, 2009

[28] S. Mohammadi, A. A. Eftekhar, and A. Adibi. "Support loss-free micro/nano-mechanical resonators using phononic crystal slab waveguides;" IEEE International Frequency Control Symposium. IEEE, 2010

[29] H. Y. Zhao, C. F. He, B. Wu, and Y. S. Wang, "Experimental realization of lower-frequency complete band gaps in 2D phononic crystals." Symposium on Piezoelectricity, Acoustic Waves and Device Applications (SPADA). IEEE, 2011.

[30] D. W. Branch, P. J. Clews, J. Nguyen, B. Kim, and P. T. Rakich, "Dispersion engineering in aluminum nitride phononic crystal plates." IEEE International Ultrasonics Symposium (IUS) IEEE, 2013.

[31] Y. Y. Chen, Y. R. Lin, T. T. Wu, and S. Y. Pao, "Anchor loss reduction of quartz resonators utilizing phononic crystals." IEEE International Ultrasonics Symposium (IUS). IEEE, 2015.

[32] Y. Deng, and Y. Jing. "Zone folding induced topological insulators in phononic crystals." IEEE International Ultrasonics Symposium (IUS). IEEE, 2017.

[33] M. Wajih Ullah Siddiqi, J. E-Y. Lee; "AlN-on-Si MEMS resonator bounded by wide acoustic bandgap two-dimensional phononic crystal anchors." IEEE Micro Electro Mechanical Systems (MEMS). IEEE, 2018.

[34] F. Bao, J. Bao, X. Li, X. Zhou, Y. Song, and X. Zhang, "Reflective strategy based on tether-integrated phononic crystals for 10 MHz MEMS resonator." Joint Conference of the IEEE International Frequency Control Symposium and European Frequency and Time Forum (EFTF/IFC). IEEE, 2019.

[35] J. Gao, X. Y. Zou, J. C. Cheng, and B. Li, "Band gaps of lower-order Lamb wave in a thin plate with one-dimensional phononic crystal layer: Effect of the substrate" Applied Physics Letters, **92** (2008) 023510.

[36] Y. Yao, F. Wu, X. Zhang, and Z. Hou, "Lamb wave band gaps in locally resonant phononic crystal strip waveguides." Physics Letters A, **376** (2012) 579.

[37] J. J. Chen, K. W. Zhang, J. Gao, and J. C. Cheng, "Stopbands for lower-order Lamb waves in one-dimensional composite thin plates." Physical Review B, **73**(2006) 094307.

[38] V. Zega, C. Gazzola, A. Buffoli, M. Conti, L. G. Falorni, G. Langfelder, A. Frangi "A defect-based MEMS phononic crystal slab waveguide." 35th IEEE International Conference on Micro Electro Mechanical Systems Conference (MEMS) 2022 Jan 9 (pp. 176-179).

[39] K. Nishimiya, T. Ohbuchi, N. Wakatsuki, K. Mizutani, and K. Yamamoto. "Visualization of negative refraction in phononic crystal using pulsed light source." IEEE International Ultrasonics Symposium, pp. 1545-1547. IEEE, 2009.

[40] F. Lucklum, and M. J. Vellekoop "Realization of complex 3-D phononic crystals with wide complete acoustic band gaps." IEEE Transactions on Ultrasonics, Ferroelectrics, and Frequency Control, **63** (2016) 796.

[41] M. Pyung Sik, K. Kim, and Y. Young Kim. "Remote beam steering with phononic crystal-based elastic waveguides;" IEEE International Ultrasonics Symposium (IUS). IEEE, 2016

[42] L. Astolfi, R. L. Watson, D. A. Hutchins, P. J. Thomas, M. Askari, A. T. Clare, L.,Nie, S. Freear, S. Laureti, and M. Ricci, "Negative refraction in conventional and additively manufactured phononic crystals." IEEE International Ultrasonics Symposium (IUS). IEEE, 2019.

[43] T. Vasileiadis, J. Varghese, V. Babacic, J. Gomis-Bresco, D. Navarro Urrios, and B. Graczykowski, "Progress and perspectives on phononic crystals." Journal of Applied Physics, **129** (2021) 160901.